Development of a Novel Ti-Nb-Au Superelastic Alloy with Exceptionally Low Elastic Modulus

NL Church, A Prasad, CEP Talbot, OG Reed, NG Jones*

Department of Materials Science and Metallurgy, University of Cambridge, 27 Charles Babbage Road, Cambridge CB3 0FS, UK

*ngj22@cam.ac.uk, Department of Materials Science and Metallurgy, University of Cambridge, 27 Charles Babbage Road, Cambridge CB3 0FS, UK

Graphical Abstract

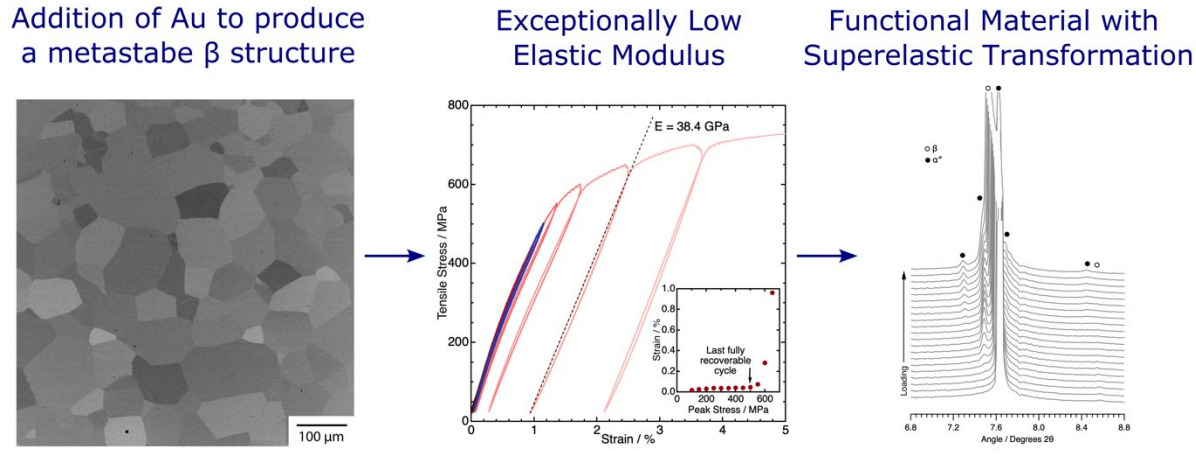

Abstract

Infection is the leading cause of biomedical implant failure, making the incorporation of antibacterial elements highly desirable. However, new alloys must also possess a low elastic modulus, to prevent stress shielding and bone resorption. Achieving this is challenging, with current alloys containing antibacterial elements being too stiff. Here, we report a novel Ti-Nb-Au alloy that contains appreciable concentrations of an antibacterial element, is free from the deleterious omega phase, has an exceptionally low elastic modulus (38.4 GPa) and high strain recoverability. These results indicate that the Ti-Nb-Au system has promise for biomedical applications, warranting further investigation and development.

Keywords

Low Modulus, Biomedical Alloy, Superelasticity, Precious Metal Additions

Impact Statement

A novel alloy from the Ti-Nb-Au system with an exceptionally low stiffness, high strain recoverability and potential for antibacterial properties is reported. This offers extraordinary potential for biomedical applications.

Titanium and its alloys are commonly used as implant materials in orthopaedic and orthodontic applications due to their biocompatibility, high corrosion resistance in biological environments and good osseointegration, which can be further improved with surface modification [1]. However, implant failures are high, affecting 10% of knee and hip arthroplasties [2] and 5-10% of dental implants [3]. Infection is cited as being the most frequent cause of implant failure in both cases [2,4], with other commonly cited causes relating to mechanical loading of the implant, resulting in bone resorption [2,3].

Bone resorption can occur due to stress shielding of the bone, when loading an implant material with high elastic modulus [5]. This eventually leads to aseptic loosening and implant failure. Currently, materials such as commercially pure (CP) titanium and Ti-6Al-4V are routinely used as implant materials, however they have moduli of ~ 110 GPa [6], which is nearly 4 times that of cortical bone (<30 GPa [7]). As such, development of new biomedical alloys has focussed on reducing the stiffness of the component materials by suitable alloying [8–11].

Transforming materials can exhibit a much lower elastic modulus than conventional elastic-plastic materials, and it is thought that this is related to the inherent lattice instability that accompanies a shear transformation [12]. Amongst this group of materials is NiTi, which has found extensive use in some biological applications. However, concerns have been raised about Ni-sensitivity of NiTi, meaning alternative low modulus materials are being explored [13].

Metastable β Ti alloys based on the Ti-Nb system have been shown to exhibit elastic moduli ranging ~ 40 - 80 GPa [14], with the values at the lower end of this range approaching that of cortical bone. The recent development of new metastable β Ti-Nb alloys, has also aimed at reducing the risk of infection of implant materials by alloying with elements such as Ag, which is known to exhibit antibacterial properties [15,16]. However, the lowest modulus achieved in Ti-Nb-Ag alloys thus far is only 68 GPa [16], which remains more than double that of cortical bone. As such, a Ti-Nb alloy that can combine both a very low elastic modulus, and the potential for enhanced antibacterial properties, would be a significant advantage in limiting implant failures.

Other metallic elements known to possess antibacterial properties include Cu [17,18] and Au [19]. Whilst Cu has been successfully incorporated into Ti-Nb based alloys to produce transforming materials [20], these alloys typically accumulate large amounts of plastic strain on loading, with shape recovery only seen following heating. Human bone on the other hand can achieve recoverable strains on the order of ~2% [14]. Furthermore, other studies on Ti-Nb-Cu alloys have demonstrated an increased modulus compared to binary Ti-Nb [21], meaning other systems should also be explored. Au is already widely used in the dental industry due to its biocompatibility and improved corrosion properties [22], and can also have the added benefit of enhancing the signal during X-ray radiography of the implant material [23]. Au has previously been added to Ti-Au-Cr-Ta alloys [23] which exhibited superelastic properties, whereby the β phase reversibly transforms to a martensite on application of a load. This reversible transformation has been shown to increase the maximum strain recoverability of the material to close to 3% in some systems [8]. However, these Au containing alloys also precipitated Ti_3Au during heat treatment, which has previously been linked to a reduction in corrosion resistance [22].

To the authors best knowledge, incorporation of Au into a Ti-Nb based superelastic alloy has not yet been reported. As such, this work presents a new Ti-Nb-Au alloy with exceptionally low elastic modulus, and recoverable superelastic behaviour, with the potential for antibacterial properties.

An ingot with a nominal composition of Ti-18Nb-4Au (at.%) was prepared by arc melting high purity elements on a water-cooled Cu hearth under an inert Ar atmosphere. The ingot was inverted and remelted five times to enhance macroscopic elemental homogeneity across the bar. 7 mm cross-sectional slices were cut from the bar and subsequently cold rolled to a final thickness of ~ 0.5 mm.

Tensile samples were prepared by electro-discharge machining (EDM) from the rolled strip, with a gauge cross section of 0.5×0.5 mm^2. Samples were sealed in evacuated quartz ampoules and heat treated at 1000°C for 5 min, before being quenched into ice-water. Short heat treatment times have previously been shown to improve superelastic properties by preventing extensive grain growth and hence increasing the yield stress [24], and strain recoverability [25].

Samples for microstructural characterisation were mounted in phenolic resin and ground using SiC papers. Final polishing was achieved to a 0.04 μm finish using colloidal silica, buffered with H_2O_2 to pH 7. Images were acquired in a GeminiSEM 300 electron microscope using a 60 μm aperture, an accelerating voltage of 15 kV and a back scattered electron (BSE) detector, configured to optimise channelling contrast.

Samples were mechanically tested *ex situ* on an Instron 3367B test frame, with a 30 kN load cell and a 12.5 mm Epsilon contact extensometer. Incremental stress tests were performed at a rate of 4 MPa s^{-1}, in increments of 50 MPa. This involved loading the sample to 50 MPa, and unloading, followed by loading to a higher stress of 100 MPa and unloading. This was repeated to higher stresses until failure of the material.

An incremental stress test was also performed on a fresh sample *in situ* on the I12 beamline at Diamond Light Source [26] with a monochromatic X-ray beam (λ = 0.1543 Å) in transmission Debye Scherrer configuration. Samples were loaded in displacement control at 4 μm s^{-1} in a Linkam TST350. The X-ray energy and experimental geometry were calibrated with a CeO_2 NIST standard sample at multiple sample to detector distances [27]. 2D Synchrotron X-ray diffraction (sXRD) images were acquired continuously, with an exposure time of 1 s per frame, using a CdTe 2M Pilatus area detector [28]. Data were reduced to 1D using the DAWN software package [29,30] by azimuthally integrating 10° segments aligned with the tensile axis. The two segments were summed to generate the 1D sXRD patterns.

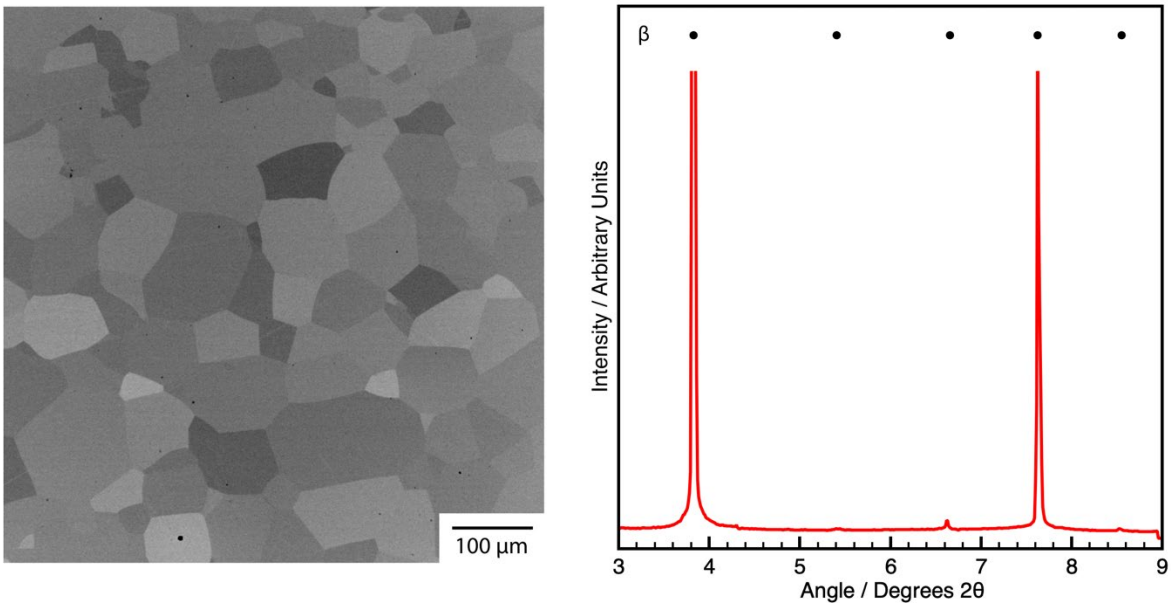

Figure 1. The initial microstructural condition of the alloy, showing recrystallised β grains and the sXRD pattern confirming the sample is single phase β.

The initial microstructural condition of the alloy following solution heat treatment is shown in Figure 1 . The micrograph highlighted recrystallised equiaxed grains on the order of ~ 80 µm. The sXRD pattern comprised intense reflections consistent with the BCC β phase. There were no reflections relating to the orthorhombic α″ or Ti_3Au intermetallic precipitates. The pattern also highlighted the absence of the ω phase, which is present in most metastable β alloys after solution treatment and rapid cooling, due to a planar collapse of the β structure to produce a hexagonal cell. ω is routinely observed using sXRD techniques [31–34], and its presence has been linked to an increased modulus in Ti-Nb alloys [8,35]. However, these data show that the Ti-18Nb-4Au (at.%) samples were single phase β prior to mechanical testing.

The *ex situ* mechanical testing data from an incremental stress test is given in Figure 2a. On loading during the first three cycles to 50, 100 and 150 MPa respectively, the sample behaved in a linear-elastic manner. When loading to 200 MPa, the sample initially displayed linear-elastic loading, however, above ~ 150 MPa, there was some deviation from linear behaviour. This was consistent with a stress induced transformation from β to α″ martensite, commonly observed in the literature for Ti-Nb containing alloys [36–38].

On unloading the sample, the strain was fully recovered, suggesting the β - α″ transformation was completely reversible on cycling to this stress. This is shown in the inset to the figure, which plots the residual plastic strain on unloading from the peak stress of each cycle.

On loading to higher stresses, the same behaviour was observed, with the cycles recovering all the applied strain up to a peak stress of 500 MPa. This cycle is shown in blue in the figure. The hysteretic loading behaviour of the β to α″ transformation could only just be seen in this cycle, Figure 2b, highlighting very low energy dissipation during loading and unloading, which is in contrast to many other Ti-Nb alloys [39,40]. The measured energy dissipation, ΔW, is 133 kJ m^{-3}, which is only half of that of

commercial biomedical alloy Ti2448 (Ti-24Nb-4Zr-8Sn, wt%), despite being loaded to twice the applied stress [39]. In the related literature for NiTi, alloys with zero, or near zero mechanical hysteresis have been linked with much better cyclic stability than their wide hysteresis counterparts [41].

Figure 2c shows the sXRD data prior to loading, and at peak load for the cycle to 500 MPa. The peak area of the β phase was considered in both cases, to give information regarding the extent of the superelastic transformation. For this specific grain orientation aligned along the tensile axis, the β peak area decreased to 41% relative intensity. However, this value is a significant underestimate of the true volume fraction of β at peak load, due to the textured nature of the α'', and elastic deformation of the β which may change the grains being sampled.

On loading to higher stresses, the sample began to accumulate some plastic strain. It has previously been demonstrated that the reversibility of the transformation is sensitive to the applied load, with alloys that are highly reversible at low applied stresses, accumulating α'' after loading to higher stresses [36].

When loading to stresses in excess of 600 MPa, the stress-strain behaviour was once again approximately linear, as shown by the black dashed line in Figure 2. This linear region was used to calculate the Young's modulus of the sample, of 38.4 GPa. This modulus is not only amongst the lowest achieved for fully dense biocompatible alloys, this has been achieved alongside fully recoverable behaviour up to 500 MPa. Other alloys which have a modulus < 40 GPa include Ti-15Nb-5.5Sn [14], Ti-5Nb-3Fe-4Sn [42], and Ti-11Nb-38Zr [43] but the superelastic recovery in these systems under ambient conditions is either low or untested. Therefore, the new Au containing alloy reported here has the potential to dramatically improve on the mechanical performance of other very low modulus structures.

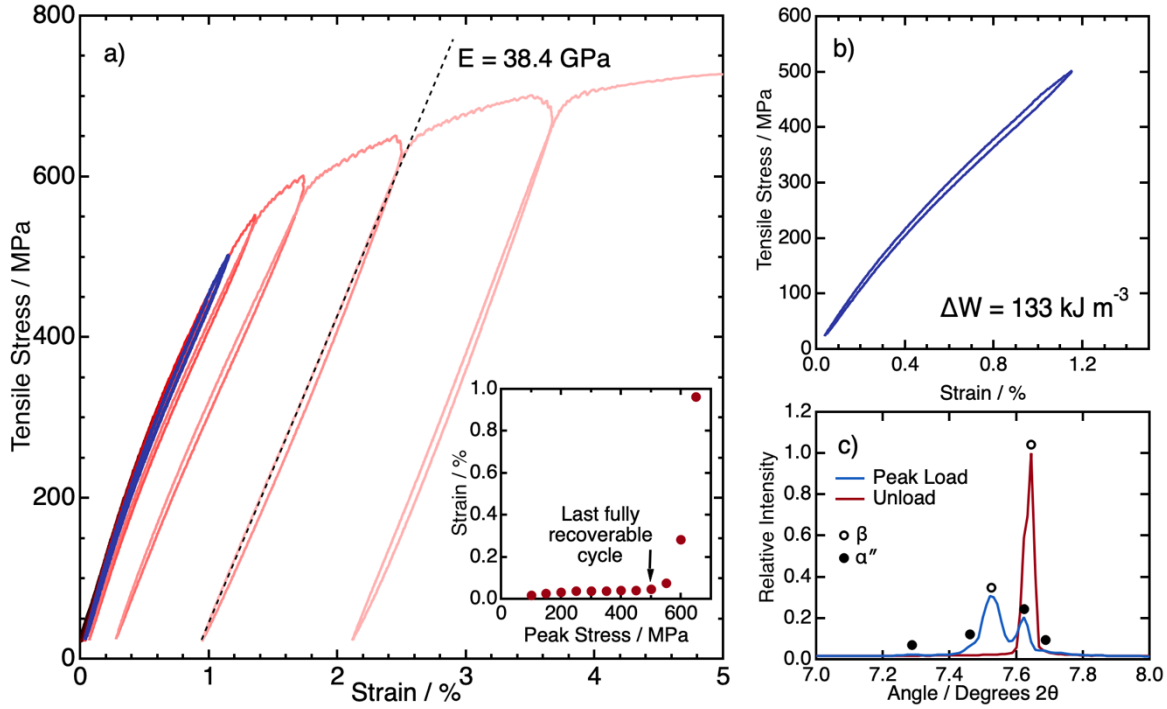

Figure 2. a) Mechanical testing data for the alloy showing an incremental stress test to failure. The strain on unload is shown in the inset to the figure, indicating the last fully recoverable cycle. This cycle to 500 MPa is shown in blue. b) The cycle to 500 MPa, highlighting the narrow hysteresis and complete recovery. c) The sXRD patterns before loading and at peak load for the cycle to 500 MPa.

To confirm that the reverse transformation was complete to 500 MPa, with no retained α'' in the microstructure, the incremental stress test was repeated *in situ*. Data following unloading for each cycle up to a peak stress of 550 MPa are shown in Figure 3. Reflections consistent with the β phase can be seen at 2θ ~7.75 and ~8.65 which correspond to the $\{022\}_\beta$ and $\{013\}_\beta$ reflections respectively. Only, following unloading from 550 MPa, can additional reflections be observed, consistent with α''. This is in good agreement with the *ex situ* mechanical data, and confirms that the cycle to 500 MPa was the last fully recoverable cycle. This was a much greater stress than is

typically experienced during mechanical loading of bone when running or walking [44], and as such this alloy is likely to be suitable for load bearing applications.

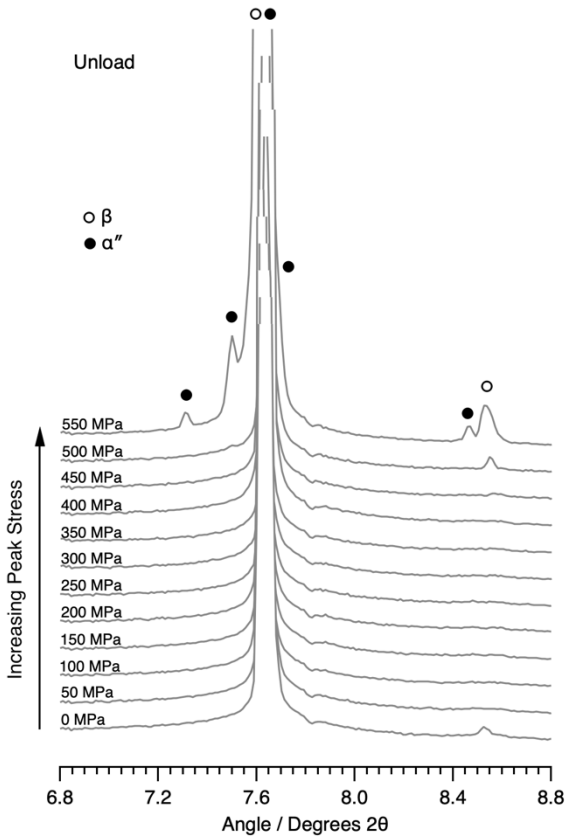

Figure 3. The sXRD diffraction patterns at unload, following each cycle in the incremental stress test. Retained α'' is seen in the microstructure following the cycle to 550 MPa.

As such, the cycle to 500 MPa was considered in more detail. The diffraction patterns during loading and unloading for this cycle are shown in Figure 4. The sample initially contained reflections for the β phase only. On loading, reflections consistent with α'' began to become discernible from the baseline. These reflections increased in intensity up to the peak load of 500 MPa. On unloading, the peaks consistent with the α'' decreased in intensity, indicating a reverse transformation from α'' to β. When fully unloaded, the α'' peaks could no longer be distinguished from the baseline, and the sample was once again single phase β. This is clear evidence of a reversible martensitic transformation suggesting an inherent instability in the β phase, which has been suggested as important for achieving a low modulus [12]. Another factor considered important for the development of a low modulus Ti-Nb based alloy is the absence of the ω phase, which can also be linked to β phase stability.

Within the literature, a number of approaches have been employed to try and predict the β phase stability, including Mo equivalency (Mo_{eq}), $\bar{B}_o - \bar{M}_d$ calculations and valence electron to atom ratio (e/a). Mo_{eq} typically requires experimental data in order to compare the β stabilising effect of different elements, which restricts its use when expanding into new alloy systems with unusual additions, such as Au. In contrast, theoretical approaches based on the electronic structure of different alloying additions can be readily extended to new systems.

$\bar{B}_o - \bar{M}_d$ maps have been used to predict the stable phases and deformation behaviour of alloys based on their composition, with many superelastic alloys falling within well-defined regions. It is thought that ω forms readily for alloys close to the slip/twin boundary [45], with other alloys sensitive to ω formation expected to exhibit superelastic behaviour. However, many superelastic compositions have been reported that do not adhere to the classically defined region for such deformation behaviour. These include Ti-Nb-Sn and Ti-Zr-Nb-Sn alloys, which are known to possess both superelastic properties and a low elastic modulus due to ω phase suppression [14,46,47]. $\bar{B}_o - \bar{M}_d$ calculations on the current alloy gives values of 2.81 and 2.35 for $\bar{B}_o$ and $\bar{M}_d$ respectively, with these values meaning the alloy also falls outside of the region of $\bar{B}_o - \bar{M}_d$ space where superelastic properties are expected. Such examples serve to highlight the caution that needs to be exercised when using these maps to determine behaviour.

In contrast, the e/a ratio has been used successfully in the design of low modulus biomedical alloys such as the commercial alloy Ti2448 (Ti-24Nb-4Zr-8Sn, wt%) [48], and Ti-15Nb-5.5Sn (at.%) [14]. The lowest modulus compositions are predicted to exist in an e/a range of approx. 4.06 – 4.15 [49], with some studies citing 4.15 as the ideal value [48]. The lower limit of this range corresponds to the presence of α″ in the initial microstructure, which is undesirable as it would be expected to increase the modulus. However, in the present study, the alloy has an e/a ratio of 4.06, whilst still retaining a metastable β microstructure.

Recent developments in the theories of the β to α″ transformation have suggested that it is not solely governed by composition and may also contain an additional driving force based on the prior processing route. One such processing variable is the cooling rate from the β phase, where samples that were quenched directly into water transformed to α″ [50]. In contrast, slower cooled samples (where ampoules remained intact, such as in the present study) were able to maintain a β phase microstructure. Optimum e/a ratios have historically been validated by studies on quenched specimens [51], and as such lower e/a ratios may allow even lower moduli to be achieved in slower cooled samples.

However, achieving a low modulus structure still relies on effective suppression of the ω phase with other very low modulus Ti-Nb alloys achieving this through the addition of Sn [14, 52]. Whilst no model currently exists for predicting alternative alloying elements that can effectively suppress ω formation, the current work has identified that this can be achieved through the addition of Au, which appears to be effective at limiting ω in the quenched microstructure. This was validated experimentally from the sXRD pattern in Figure 1, with sXRD techniques routinely used to detect even low volume fractions of the ω phase [32,53,54]. Therefore, despite current predictive tools being insufficient to capture the behaviour of this system, the combination of low β stability, and limited ω phase formation rationalises the low modulus achieved in this alloy.

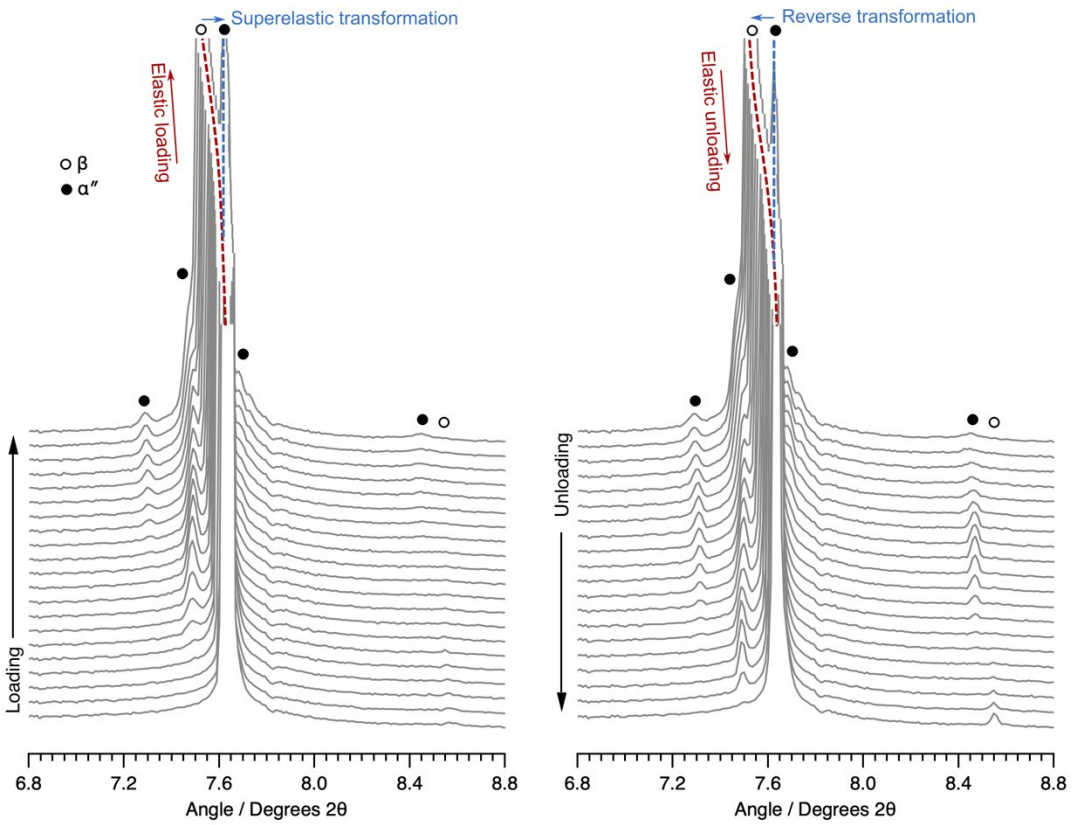

Figure 4. sXRD patters during loading and unloading to 500 MPa, which is the last fully recoverable superelastic cycle. The coloured lines show the shift in β peak position due to elastic deformation, and the peak splitting due to the transformation to α''.

In summary, an ω free Ti-Nb-Au alloy has been successfully produced with an exceptionally low elastic modulus of 38.4 GPa for a fully dense structure. The incorporation of Au provides the potential for enhanced corrosion properties, improved X-ray signal, and antibacterial properties. This is the first time an alloy has been reported, with the combination of a low elastic modulus approaching that of human bone, good strain recovery and the potential for antibacterial properties. As such, this alloy has the potential to address the two leading causes for implant failure in both orthodontic and orthopaedic applications. These results indicate that the Ti-Nb-Au system has great promise as a new solution for biomedical implant applications. Further, more extensive, studies are clearly warranted to develop an optimised Ti-Nb-Au superelastic alloy and establish its antibacterial properties.

Credit statement

NL Church: Methodology; Investigation; Formal analysis; Validation; Writing – original draft; Visualization. A Prasad: Investigation. CEP Talbot: Investigation. OG Reed: Investigation. NG Jones: Conceptualization; Methodology; Investigation; Validation; Formal analysis; Writing – original draft; Resources; Supervision; Project administration; Funding acquisition.

Data Availability

The underlying research data required to reproduce these findings are available from the University of Cambridge repository (10.17863/CAM.100116)

Acknowledgements

The authors would like to acknowledge the Goldsmiths' Company Assay Office, London and the EPSRC (EP/511870/1 & EP/R513180/1) for supporting this research. Beam time was provided by Diamond Light Source under MG31965.

Declaration of competing interest

The authors declare that they have no known competing financial interests or personal relationships that could have appeared to influence the work reported in this paper.

References

1. Gajiwala M, Paliwal J, Husain SY, Dadarwal A, Kalla R, Sharma V, Sharma M. Influence of surface modification of titanium implants on improving osseointegration: An in vitro study.
2. Raphel J, Holodniy M, Goodman SB, Heilshorn SC. Multifunctional coatings to simultaneously promote osseointegration and prevent infection of orthopaedic implants. Vol. 84, Biomaterials. Elsevier Ltd; 2016. p. 301–14.
3. Tabanella G, Nowzari H, Slots J. Clinical and microbiological determinants of ailing dental implants. Clin Implant Dent Relat Res. 2009 Mar;11(1):24–36.
4. Kochar SP, Reche A, Paul P. The Etiology and Management of Dental Implant Failure: A Review. Cureus. 2022 Oct 19;
5. Anijs T, Kouwert I, Verdonschot N, Janssen D. Towards a Standard Approach to Assess Tibial Bone Loss Following Total Knee Arthroplasty. Vol. 18, Clinical Reviews in Bone and Mineral Metabolism. Springer; 2020. p. 72–86.
6. Martins JRS, Araújo RO, Nogueira RA, Grandini CR. Internal friction and microstructure of ti and ti-mo alloys containing oxygen. Archives of Metallurgy and Materials. 2016;61(1):25–30.
7. Wilson J. Metallic biomaterials. In: Fundamental Biomaterials: Metals. Elsevier; 2018. p. 1–33.
8. Yang R, Hao YL, Li SJ. Development and Application of Low-Modulus Biomedical Titanium Alloy Ti2448. In: Biomedical Engineering, Trends in Materials Science [Internet]. 2011 [cited 2018 Oct 29]. p. 225–48. Available from: www.intechopen.com
9. Matsumoto H, Watanabe S, Hanada S. Beta TiNbSn Alloys with Low Young's Modulus and High Strength [Internet]. Vol. 46, Materials Transactions. 2005 [cited 2018 Oct 10]. Available from: https://www.jstage.jst.go.jp/article/matertrans/46/5/46_5_1070/_article
10. Ikehata H, Nagasako N, Furuta T, Fukumoto A, Miwa K, Saito T. First-principles calculations for development of low elastic modulus Ti alloys. Phys Rev B [Internet]. 2004;70(17):174113. Available from: https://link.aps.org/doi/10.1103/PhysRevB.70.174113
11. Hao YL, Li SJ, Prima F, Yang R. Controlling reversible martensitic transformation in titanium alloys with high strength and low elastic modulus. Scr Mater. 2012;67(5):487–90.
12. Kim HY, Miyazaki S. Ni-Free Ti-Based Shape Memory Alloys. Elsevier; 2018.

13. Miyazaki S, Kim HY, Hosoda H. Development and characterization of Ni-free Ti-base shape memory and superelastic alloys. Materials Science and Engineering A [Internet]. 2006 [cited 2018 Mar 18];438–440(SPEC. ISS.):18–24. Available from: https://ac.els-cdn.com/S0921509306005594/1-s2.0-S0921509306005594-main.pdf?_tid=bfb3fe7d-4a1d-483f-9269-844d8cd68cdd&acdnat=1521395175_8381cc3afec9729723ef379cf847b530
14. Li S, Lee WT, Yeom JT, Kim JG, Oh JS, Lee T, Liu Y, Nam TH. Towards bone-like elastic modulus in Ti-Nb-Sn alloys with large recovery strain for biomedical applications. J Alloys Compd. 2022 Dec 5;925:166724.
15. Hussein MA, Kumar AM, Azeem MA, Sorour AA, Saravanan S. Ti–30Nb–3Ag alloy with improved corrosion resistance and antibacterial properties for orthopedic and dental applications produced by mechanical alloying. J Mech Behav Biomed Mater. 2023 Jun 1;142.
16. Hussein MA, Azeem MA, Kumar AM, Saravanan S, Ankah N, Sorour AA. Design and processing of near-β Ti–Nb–Ag alloy with low elastic modulus and enhanced corrosion resistance for orthopedic implants. Journal of Materials Research and Technology. 2023 May;24:259–73.
17. Zhang E, Zhao X, Hu J, Wang R, Fu S, Qin G. Antibacterial metals and alloys for potential biomedical implants. Vol. 6, Bioactive Materials. KeAi Communications Co.; 2021. p. 2569–612.
18. Zhao Z, Xu W, Xin H, Yu F. Microstructure, corrosion and anti-bacterial investigation of novel Ti-xNb-yCu alloy for biomedical implant application. Journal of Materials Research and Technology. 2022 May 1;18:5212–25.
19. Fu S, Zhao X, Yang L, Qin G, Zhang E. A novel Ti-Au alloy with strong antibacterial properties and excellent biocompatibility for biomedical application. Biomaterials Advances. 2022 Feb 1;133.
20. Horiuchi Y, Nakayama K, Inamura T, Kim HY, Wakashima K, Miyazaki S, Hosoda H. Effect of Cu addition on shape memory behavior of Ti-18 mol%Nb alloys. Mater Trans. 2007 Mar;48(3):414–21.
21. Alberta LA, Vishnu J, Hariharan A, Pilz S, Gebert A, Calin M. Novel low modulus beta-type Ti-Nb alloys by gallium and copper minor additions for antibacterial implant applications. Journal of Materials Research and Technology. 2022 Sep 1;20:3306–22.
22. Takahashi M, Kikuchi M, Takada Y, Okuno O, Okabe T. Corrosion Behavior and Microstructures of Experimental Ti-Au Alloys. Dent Mater J. 2004;23(2):109–16.
23. Chiu WT, Fuchiwaki K, Umise A, Tahara M, Inamura T, Hosoda H. Enhancement of the superelastic behavior of the Ti–Au–Cr–based shape memory alloys via the manipulations of annealing–treatments and Ta additions. Materials Science and Engineering: A. 2022 Jul 7;847.
24. Church NL, Hildyard EM, Jones NG. The influence of grain size on the onset of the superelastic transformation in Ti–24Nb–4Sn–8Zr (wt%). Materials Science and Engineering A [Internet]. 2021;828(July):142072. Available from: https://doi.org/10.1016/j.msea.2021.142072
25. Gao JJ, Thibon I, Castany P, Gloriant T. Effect of grain size on the recovery strain in a new Ti–20Zr–12Nb–2Sn superelastic alloy. Materials Science and Engineering A [Internet]. 2020;793(July):139878. Available from: https://doi.org/10.1016/j.msea.2020.139878

26. Drakopoulos M, Connolley T, Reinhard C, Atwood R, Magdysyuk O, Vo N, Hart M, Connor L, Humphreys B, Howell G, Davies S, Hill T, Wilkin G, Pedersen U, Foster A, De Maio N, Basham M, Yuan F, Wanelik K. I12: The Joint Engineering, Environment and Processing (JEEP) beamline at Diamond Light Source. J Synchrotron Radiat. 2015 May 1;22:828–38.
27. Hart ML, Drakopoulos M, Reinhard C, Connolley T. Complete elliptical ring geometry provides energy and instrument calibration for synchrotron-based two-dimensional X-ray diffraction. J Appl Crystallogr. 2013 Oct;46(5):1249–60.
28. Šišak Jung D, Donath T, Magdysyuk O, Bednarcik J. High-energy X-ray applications: current status and new opportunities. Powder Diffr. 2017 Dec;32(S2):S22–7.
29. Filik J, Ashton AW, Chang PCY, Chater PA, Day SJ, Drakopoulos M, Gerring MW, Hart ML, Magdysyuk O V., Michalik S, Smith A, Tang CC, Terrill NJ, Wharmby MT, Wilhelm H. Processing two-dimensional X-ray diffraction and small-angle scattering data in DAWN 2. J Appl Crystallogr. 2017 Jun 1;50(3):959–66.
30. Basham M, Filik J, Wharmby MT, Chang PCY, El Kassaby B, Gerring M, Aishima J, Levik K, Pulford BCA, Sikharulidze I, Sneddon D, Webber M, Dhesi SS, Maccherozzi F, Svensson O, Brockhauser S, Náray G, Ashton AW. Data Analysis WorkbeNch (DAWN). J Synchrotron Radiat. 2015;22:853–8.
31. Hildyard EM, Connor LD, Owen LR, Rugg D, Martin N, Stone HJ, Jones NG. The influence of microstructural condition on the phase transformations in Ti-24Nb (at.%). Acta Mater [Internet]. 2020;199:129–40. Available from: https://doi.org/10.1016/j.actamat.2020.08.004
32. Zhang J, Sun F, Hao Y, Gozdecki N, Lebrun E, Vermaut P, Portier R, Gloriant T, Laheurte P, Prima F. Influence of equiatomic Zr/Nb substitution on superelastic behavior of Ti-Nb-Zr alloy. Materials Science and Engineering A. 2013;563:78–85.
33. Elmay W, Prima F, Gloriant T, Bolle B, Zhong Y, Patoor E, Laheurte P. Effects of thermomechanical process on the microstructure and mechanical properties of a fully martensitic titanium-based biomedical alloy. J Mech Behav Biomed Mater [Internet]. 2013;18:47–56. Available from: http://dx.doi.org/10.1016/j.jmbbm.2012.10.018
34. Ijaz MF, Kim HY, Hosoda H, Miyazaki S. Effect of Sn addition on stress hysteresis and superelastic properties of a Ti-15Nb-3Mo alloy. Scr Mater [Internet]. 2014 Feb 1 [cited 2019 Oct 1];72–73:29–32. Available from: https://www.sciencedirect.com/science/article/pii/S1359646213005058
35. Bönisch M, Calin M, Van Humbeeck J, Skrotzki W, Eckert J. Factors influencing the elastic moduli, reversible strains and hysteresis loops in martensitic Ti-Nb alloys. Materials Science and Engineering C. 2015 Mar 1;48:511–20.
36. Church NL, Jones NG. The influence of stress on subsequent superelastic behaviour in Ti2448 (Ti–24Nb–4Zr–8Sn, wt%). Materials Science and Engineering: A [Internet]. 2021;833(October 2021):142530. Available from: https://doi.org/10.1016/j.msea.2021.142530
37. Kim HY, Ohmatsu Y, Kim JI, Hosoda H, Miyazaki S. Mechanical Properties and Shape Memory Behavior of Ti-Nb Alloys. Mater Trans [Internet]. 2004 [cited 2017 Oct 15];45(4):1090–5. Available from: https://www.jim.or.jp/journal/e/pdf3/45/07/2443.pdf
38. Héraud L, Castany P, Ijaz MF, Gordin DM, Gloriant T. Large-strain functional fatigue properties of superelastic metastable β titanium and NiTi alloys: A comparative study. J Alloys Compd. 2023 Aug 25;953.

39. Church N, Talbot C, Connor L, Michalik S, Jones N. Functional fatigue during superelastic load cycling of Ti2448 (Ti-24Nb-4Zr-8Sn, wt%). Materialia (Oxf) [Internet]. 2023 May;28:101719. Available from: https://linkinghub.elsevier.com/retrieve/pii/S2589152923000479
40. Vorontsov VA, Jones NG, Rahman KM, Dye D. Superelastic load cycling of Gum Metal. Acta Mater [Internet]. 2015 [cited 2017 Oct 8];88:323–33. Available from: https://ac.els-cdn.com/S1359645415000464/1-s2.0-S1359645415000464-main.pdf?_tid=0e76ff62-ac38-11e7-9b0f-00000aab0f26&acdnat=1507474422_429c6a45baab9efb6abfc3d571b9d784
41. Tong Y, Shuitcev A, Zheng Y. Recent Development of TiNi-Based Shape Memory Alloys with High Cycle Stability and High Transformation Temperature. Vol. 22, Advanced Engineering Materials. Wiley-VCH Verlag; 2020.
42. Farzik Ijaz M, Tasaki W, Young Kim H, Miyazaki S. Achievement of ultra-low elastic modulus through optimization of phase stability and recrystallization texture in Ti–Nb–Fe–Sn alloys. Adv Eng Mater. 2023 Jul 12;2300468.
43. You L, Song X. A study of low Young's modulus Ti-Nb-Zr alloys using d electrons alloy theory. Scr Mater. 2012 Jul;67(1):57–60.
44. Meardon SA, Derrick TR, Willson JD, Baggaley M, Steinbaker CR, Marshall M, Willy RW. Peak and Per-Step Tibial Bone Stress During Walking and Running in Female and Male Recreational Runners. American Journal of Sports Medicine. 2021 Jul 1;49(8):2227–37.
45. Morinaga M, Kato M, Kamimura T, Fukumoto M, Harada I, Kubo K. Theoretical Design of b-type Titanium Alloys. The Minerals, Metals & Materials Society. 1993;
46. Cai S, Wang L, Schaffer JE, Gao J, Ren Y. Influence of Sn on martensitic beta Ti alloys. Materials Science and Engineering: A. 2019 Jan 16;743:764–72.
47. Fu J, Yamamoto A, Kim HY, Hosoda H, Miyazaki S. Novel Ti-base superelastic alloys with large recovery strain and excellent biocompatibility. Acta Biomater. 2015 Apr 15;17:56–67.
48. Hao YL, Li SJ, Sun SY, Zheng CY, Yang R. Elastic deformation behaviour of Ti-24Nb-4Zr-7.9Sn for biomedical applications. Acta Biomater [Internet]. 2007 Mar 1 [cited 2018 Oct 9];3(2):277–86. Available from: https://www.sciencedirect.com/science/article/pii/S1742706106001528
49. Luke CA, Taggart R, Polonis DH. Electronic Factors and the Metastable Constitution of Quenched Alloys based on Titanium and Zirconium.
50. Church NL, Talbot CEP, Jones NG. On the Influence of Thermal History on the Martensitic Transformation in Ti-24Nb-4Zr-8Sn (wt%). Shape Memory and Superelasticity [Internet]. 2021;7(1):166–78. Available from: https://doi.org/10.1007/s40830-021-00309-2
51. Fedotov SV, Baikov AA. Peculiarities of Changes in Elastic Properties of Titanium Alloys. In: Jeffee, Burte, editors. Titanium Science and Technology. 1973. p. 871–81.
52. Hao YL, Li SJ, Sun SY, Yang R. Effect of Zr and Sn on Young's modulus and superelasticity of Ti-Nb-based alloys. Materials Science and Engineering A [Internet]. 2006 Dec 15 [cited 2018 Oct 8];441(1–2):112–8. Available from: https://www.sciencedirect.com/science/article/pii/S0921509306020351
53. Figueiredo Azevedo T, Nunes Lima T, Garcia de Blas J, Carlos Pereira L, Griza S. The mechanical behavior of TiNbSn alloys according to alloying contents, cold rolling and aging. J Mech Behav Biomed Mater. 2017;75:33–40.

493 54. Al-Zain Y, Kim HY, Hosoda H, Nam TH, Miyazaki S. Shape memory properties of Ti-Nb-
494 Mo biomedical alloys. Acta Mater [Internet]. 2010;58(12):4212–23. Available from:
495 http://dx.doi.org/10.1016/j.actamat.2010.04.013
496